

# Synthesis of Silica–Gold Nanocomposites and Their Porous Nanoparticles by an In-Situ Approach

Ashavani Kumar,<sup>†,\*</sup> Victor L. Pushparaj,<sup>†,\*</sup> Saravanababu Murugesan,<sup>‡</sup>  
 Gunaranjan Viswanathan,<sup>†</sup> Rohit Nalamasu,<sup>†,§</sup> Robert J. Linhardt,<sup>‡</sup>  
 Omkaram Nalamasu,<sup>†</sup> and Pulickel M. Ajayan<sup>†</sup>

*Department of Materials Science and Engineering and Department of Chemical and Biological Engineering, Rensselaer Polytechnic Institute, Troy, New York 12180 and Niskayuna High School, Ball Town Road, Niskayuna, New York 12309*

*Received March 31, 2006. In Final Form: August 13, 2006*

We demonstrate the one-step synthesis of a silica–gold nanocomposite by simultaneous hydrolysis and reduction of gold chloride. The aminophenyl group was used as a reducing agent, and the trimethoxy silane group acts a precursor for the formation of silica. The porous gold nanoparticles were formed by etching out the silica–gold nanocomposite by hydrofluoric acid. The electron diffraction of porous gold nanoparticles showed that the particles are polycrystalline with FCC structure. The silica–gold nanocomposite exhibited nonlinear current–voltage behavior, and the porous gold nanoparticles displayed linear current–voltage behavior.

## Introduction

Silica–metal composite materials have attracted a great deal of interest because of their biomedical<sup>1</sup> and catalysis<sup>2</sup> applications. There are many known methods available for synthesizing various kinds of silica–metal-based composite materials such as metal core–silica shells,<sup>3</sup> silica core–metal shells,<sup>4</sup> and nanoparticles embedded in porous silica.<sup>5</sup> These materials are useful candidates (e.g., hollow or porous materials<sup>6</sup>) for the encapsulation of drugs, different kinds of catalysis reaction, and electronic devices. Synthesis protocols of oxide–metal composite materials are already known; however, most of them are multistep processes that require a separate synthesis of metal nanoparticles and subsequent synthesis of oxide and vice versa.<sup>3–6</sup> These composite materials can be transformed into porous materials by simply etching out the silica.<sup>6</sup> Recently, Caruso et al. demonstrated this by incorporating the porous gold nanoparticles into polymer beads and thereafter removing the organic matrix.<sup>7</sup> This is a slow multistep process. Hence, it is essential to have simple, scalable protocols for the synthesis of composite materials or porous nanomaterials. Here we demonstrate the synthesis of silica–gold composite materials by in-situ reduction and hydrolysis of gold ions and silica precursors. Porous gold nanoparticles were formed by simply etching out the silica from the silica–gold

composite using hydrofluoric acid. This protocol does not require a separate synthesis of nanoparticles or any other external reducing agent.

## Experimental Section

The following chemicals were used as obtained: *N*-[3-trimethoxy-silyl-propyl]aniline (TMSPA) and hydrogen tetrachloroaurate trihydrate (chloroauric acid, H<sub>2</sub>AuCl<sub>4</sub>·3H<sub>2</sub>O) were purchased from Sigma-Aldrich Chemicals. In a typical experiment, 25 mL of TMSPA solution ( $2 \times 10^{-3}$  M) was added to 25 mL of chloroauric acid solution ( $2 \times 10^{-3}$  M), and the solution was kept in the dark and stirred for 5 h. The initially pale-yellow solution turned red. The pH of the solution was 3.5, which was increased to 8 using sodium hydroxide solution, and the solution was stirred for 12 h for reduction and complete hydrolysis of TMSPA. The silica–gold composite particles were separated by centrifuge at a speed of 3000 rpm and dispersed in double-distilled water. The porous gold nanoparticles were obtained by etching the silica from silica–gold composite particles. In a typical experiment, 20 mg of the silica–gold nanocomposite was dispersed in 50 mL of 52% concentrated hydrofluoric acid for etching out silica (duration of etching ~2 h). After etching, the particles were separated by centrifugation at a speed of 8000 rpm and were characterized by various characterization techniques.

FTIR measurements of the silica–gold composite particles and porous gold nanoparticles were carried out on a Perkin-Elmer Spectrum1 spectrometer in the diffuse reflectance mode at an 80° incident beam angle to the surface normal. UV–vis spectroscopy measurements of all the samples were performed in a Varian Cary 500 Scan UV–vis–NIR spectrophotometer operated at a resolution of 2 nm. The silica–gold nanocomposite particles and porous gold nanoparticles were drop casted on TEM grid and measurements were carried out in a CM12 transmission electron microscope operated at an accelerating voltage of 120 kV. X-ray photoelectron spectroscopy (XPS) measurements were carried out on drop coated films of nanocomposite materials and porous gold nanoparticles on copper substrate using PHI 5400 instrument (200 W Mg K $\alpha$  probe beam). The spectrometer was configured to operate at high resolution with pass energy of 20 eV.

## Result and Discussion

The silica–gold nanocomposite and porous gold nanoparticles were formed as described in the Experimental Section. Figure 1A shows the spectrum of the silica–gold composite, and the

\* Corresponding authors. E-mail: kumara4@rpi.edu (A. Kumar), pushpv@rpi.edu (P. Victor). Tel: 001-518-2768703. Fax: 001-518-2768554.

<sup>†</sup> Department of Materials Science and Engineering, Rensselaer Polytechnic Institute.

<sup>‡</sup> Department of Chemical and Biological Engineering, Rensselaer Polytechnic Institute.

<sup>§</sup> Niskayuna High School.

(1) Hirsch, L. R.; Stafford, R. J.; Bankson, J. A.; Sershen, S. R.; Rivera, B.; Price, R. E.; Hazle, J. D.; Halas, N. J.; West, J. L. *Proc. Natl. Acad. Sci.* **2003**, *100*, 13549.

(2) Visser, T.; Nijhuis, T. A.; Vander Eerden, Ad M. J.; Jenken, K.; Ji, Y.; Bras, W.; Nikitenko, S.; Ikeda, Y.; Lepage M.; Weckhuysen B. M. *J. Phys. Chem. B* **2005**, *109*, 3822.

(3) Tom, R. T.; Nair, A. S.; Singh, N.; Aslam, M.; Nagendra, C. L.; Vijayamohan, K. R.; Pradeep, T. *Langmuir* **2003**, *19*, 3439. Pastoriza-Santos, I.; Koktysh, D. S.; Mamedov, A. A.; Michael Giersig, M.; Kotov, N. A.; Liz-Marza'n, L. M. *Langmuir* **2000**, *16*, 2731

(4) Graf, C.; Blaaderen, A. V. *Langmuir* **2002**, *18*, 524. Westcott, S. L.; Oldenburg, S. J.; Lee, T. R.; Halas, N. J. *Langmuir* **1998**, *14*, 5396.

(5) Mandal, S.; Roy, D.; Chaudhari, R. V.; Sastry, M. *Chem. Mater.* **2004**, *16*, 3714

(6) Chah, S.; Fendler, J. H.; Yi, J. *J. Colloid Interface Sci.* **2002**, *250*, 142.

(7) Shchukin D. G.; Caruso R. A. *Chem. Commun.* **2003**, 1478.

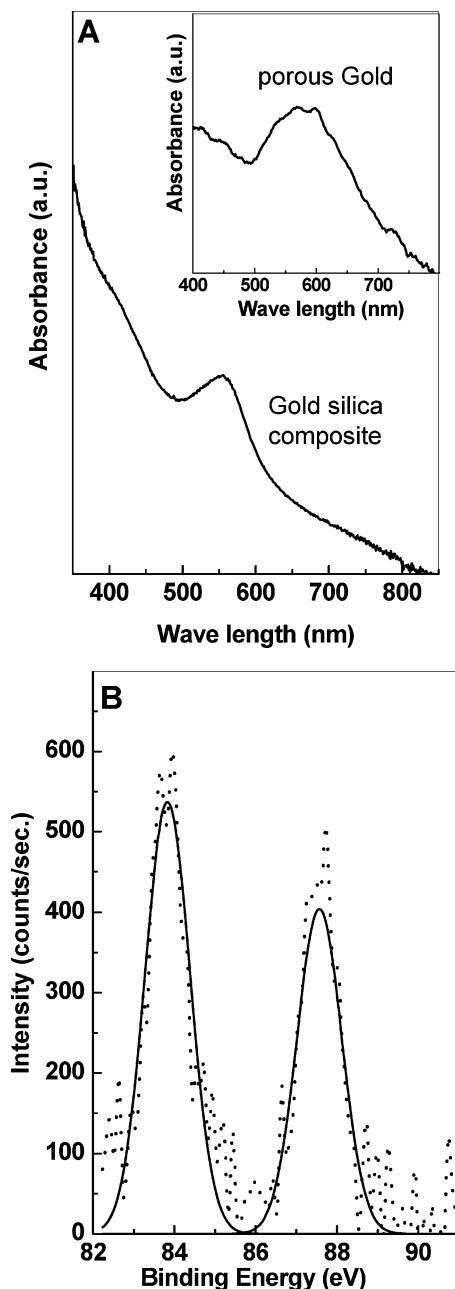


**Figure 1.** (A) UV-vis spectra of the silica-gold composite before and after (inset) treatment with HF. (B) Au 4f core-level spectra recorded from a porous gold nanoparticle film deposited on a copper substrate. The spin-orbit components are shown.

inset of Figure 1A shows the spectrum of porous gold nanoparticles that was obtained after etching with hydrofluoric acid. A strong resonance at ca. 520 nm is seen in both spectra, and this absorption band arises from the excitation of surface plasmon vibrations in the gold nanoparticles. This band indicates the formation of gold nanoparticles due to the reduction of gold ions by TMSPA molecules. The UV-vis spectra of these two nanoparticle solutions remain unchanged with time, indicating that the particle size distribution was extremely stable. The surface plasmon resonance position does not change even after removing silica, which clearly indicates that particles do not aggregate even after HF treatment.

An XPS spectrum of the Au 4f core level (Figure 1B) was recorded on the porous gold nanoparticles drop casted on the Cu substrate at room temperature. The Au 4f spectrum was resolved into a single spin-orbit pair coupling (splitting  $\sim 3.7$  eV) with a  $4f_{7/2}$  binding energy (BE) of 83.8 eV. The silica-gold composite

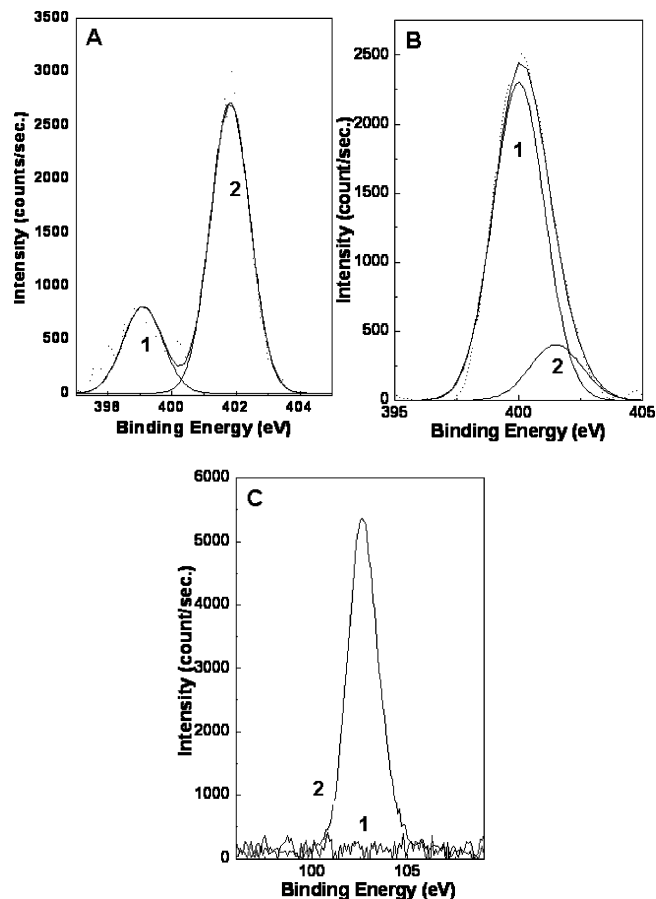


**Figure 2.** (A) N 1s core-level spectra recorded from a porous gold nanoparticle (A) and a silica-gold composite film (B) deposited on a copper substrate. (C) Si 2p core-level spectra recorded from a porous gold film (curve 1) and a silica-gold composite film (curve 2) deposited on a copper substrate.

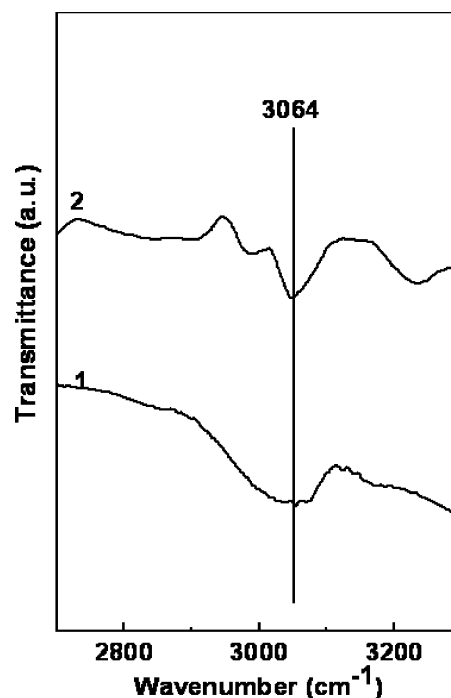


**Figure 3.** FTIR spectra of a drop-coated film of silica-gold composite particles (curve 1) and porous gold nanoparticles (curve 2) on a Si(111) substrate.

particles also show similar Au 4f spectra, and there is no evidence of additional components in the Au 4f spectrum. The binding

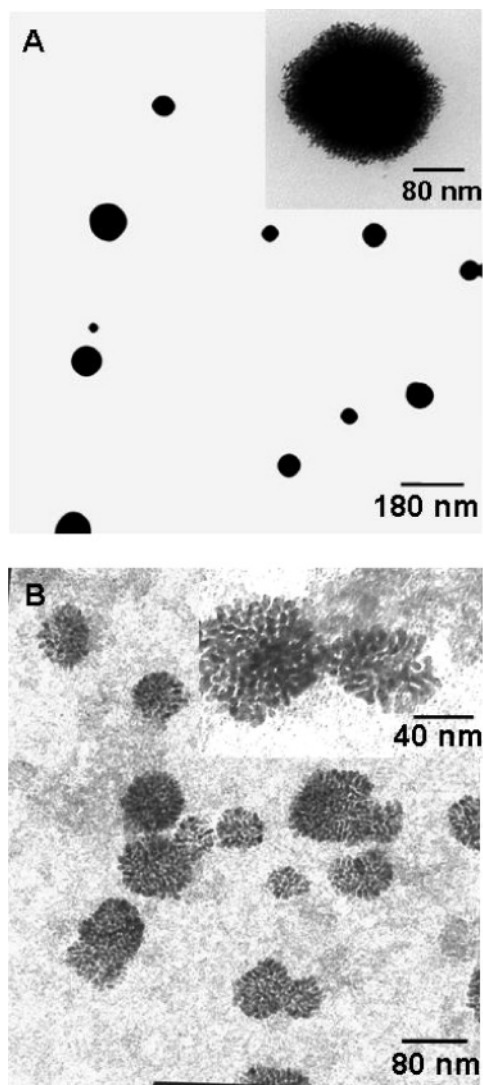


**Figure 4.** TEM image of a drop-coated film of a silica-gold composite (A) before and (B) after HF treatment on a carbon-coated copper grid.

energy of the Au 4f core level is in agreement with XPS spectra of alkylamine-capped gold nanoparticles as reported by Leff, Brandt, and Heath.<sup>8</sup> In addition to the Au 4f signal, a strong N 1s, Si 2p signal was also observed in the film, suggesting the presence of the amino group on the surface of the gold nanoparticles and silica-gold nanocomposite as shown in Figure 2A and B.

The N 1s spectrum of obtained porous gold nanoparticles and silica-gold composite materials before HF etching materials are shown in Figure 2A and B, which can be resolved into two chemically distinct species centered at 399.3 and 402 eV. The higher BE component is assigned to electron emission from nitrogen in the amine groups bonded with gold nanoparticles. We believe the lower and higher binding energy component is due to the amine and protonated amine groups attached to gold nanoparticles.<sup>9</sup> The number of protonated amine groups attached to gold is relatively larger in porous gold as compare to the number in silica-gold composite materials, which may be due to the protonation of the amine group on treating with HF for silica etching. Figure 2C shows the Si 2p core level of porous gold (curve 1) and silica-gold composite materials (curve 2). The absence of the Si 2p core level in the porous gold indicates the complete removal of silica as a result of etching. Figure 3 is the FTIR spectrum of a drop-coated film of silica-gold

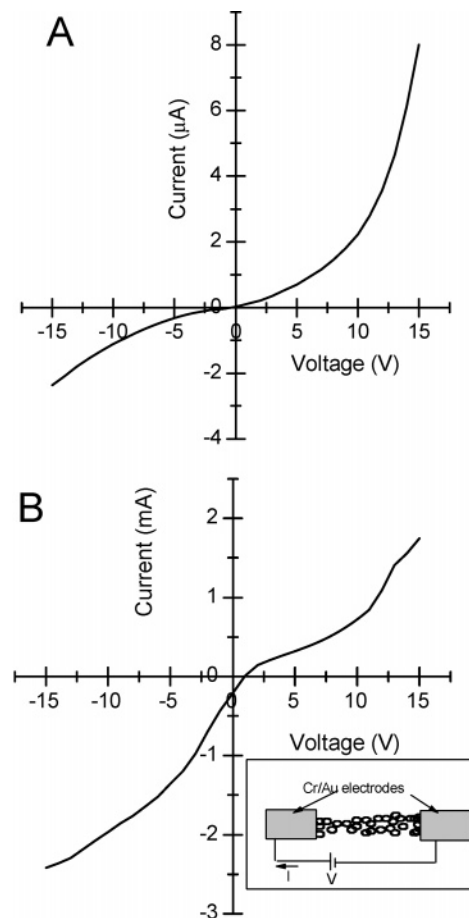


**Figure 5.**  $I$ - $V$  curves of (A) a silica-gold composite and (B) porous gold nanoparticles measured at 300 K. The inset shows a schematic of metal electrodes with nanoparticles or composite dispersed between the electrodes.

composite materials (curve 1) and porous gold (curve 2) on the Si(111) substrate. Both spectra show a prominent feature at ca.  $3064\text{ cm}^{-1}$  that corresponds to the aromatic C-H stretching vibration from the phenyl ring. The N-H peak is absent in both samples, indicating the oxidation and coordination of the aniline group to the gold nanoparticles. It is well known in the open literature that the amino phenyl group reduces the gold ions<sup>10,11</sup> and forms nanoparticles. Hence, the amino phenyl group present in TMSPA molecules plays a similar role in the synthesis of gold nanoparticles. Figure 4 shows the transmission electron microscopy image of the silica-gold composite before (Figure 4A) and after HF treatment (Figure 4B). The insets in Figure 4A and B, respectively, show their corresponding higher-magnification images. The higher-magnification image of silica-gold particles shows that the surface is quite rough and hairy. The average size of silica-gold nanocomposite materials was  $\sim 66 \pm 22\text{ nm}$ , which decreases to  $30 \pm 6\text{ nm}$  after treatment with HF. The texture of the silica-gold nanocomposite is replaced by a rough morphology with irregular pores on the surface. The decrease in particle size and the change in morphology are due to the dissolution of silica in HF. We believe that silica-gold nanocomposite materials are formed by the simultaneous hydrolysis and reduction of gold

(8) Leff, D. V.; Brandt, L.; Heath, J. R. *Langmuir* **1996**, *12*, 4723. Green, M.; O'Brien, P. *Chem. Commun.* **2000**, 183.

(9) Kumar, A.; Mandal, S.; Selvakannan, P. R.; Pasricha, R.; Mandale, A. B.; Sastry, M. *Langmuir* **2003**, *19*, 6277.

(10) Selvakannan, P. R.; Mandal, S.; Pasricha, R.; Adyanthaya, S. D.; Sastry, M. *Chem. Commun.* **2002**, 1334.

(11) Mandal, S.; Selvakannan, P. R.; Roy, D.; Chaudhari, R. V.; Sastry, M. *Chem. Commun.* **2002**, 3002.

ions. The amino phenyl group reduced the gold ion and formed nanoparticles, and the hydrolysis of the silane group is responsible for silica. The gold nanoparticles are uniformly distributed in silica particles. The presence of silica makes the surface rough, hairy, and porous. On HF treatment, the silica–gold nanoparticle structure collapses and disintegrates into a smaller structure because of silica dissolution. During this process, the gold nanoparticles partially aggregate and transform to the porous structure. This is readily observed from the XPS spectra. Electron diffraction (porous gold) obtained from TEM reveals polycrystalline nanoparticles with FCC structure.

The current–voltage ( $I$ – $V$ ) behavior of composite and porous nanoparticles was studied at different temperatures (300–373 K) on sweeping the bias voltage from  $-30$  to  $+30$  V. The sample was prepared by spin coating the nanoparticles and nanocomposites separately on the coplanar metal electrode substrates, and the schematic is shown as the inset of Figure 5B. The square ( $2\text{ mm}^2$  area) coplanar electrodes were patterned by a photolithography technique at a separation of 1 mm between the metal electrodes. The metal (20 nm Cr/50 nm Au) electrode was deposited by e-beam evaporation on  $\text{SiO}_2/\text{Si}$  substrates.  $I$ – $V$  curves measured at room temperature of the silica–gold nanocomposite and porous gold nanoparticles are shown in Figure 5A and B, respectively. The resistance values measured at 300 K were  $25\text{ M}\Omega$  and  $5\text{ k}\Omega$  for the silica–gold composite and porous gold nanoparticles, respectively. The porous gold nanoparticles exhibited nearly linear  $I$ – $V$  behavior, and the silica–gold composite exhibited nonlinear asymmetrical behavior. The latter behavior is due to the presence of silica, which is an insulator,

and it is interesting to observe the nonlinear asymmetrical behavior that shows a slight trend of rectification behavior (i.e., at reverse bias the current remains low even at higher voltages). This is different from the earlier report that shows that they do show linear behavior in the gold nanocrystal/silica arrays.<sup>12</sup> The  $I$ – $V$  measurement carried at higher temperatures ( $>300\text{ K}$ ) does show a steady increase in the current in the case of nanocomposites, indicating that electrical conduction is also activated thermally. The slight rectification behavior in gold–silica nanocomposites will definitely be of interest for electronic devices (e.g., nanorectifier devices).

In summary, we have demonstrated a new approach to the synthesis of silica–gold nanocomposites in a single step using an in-situ reduction approach. This composite material was then used to make porous gold nanoparticles using HF. The current–voltage curves on the nanocomposite show nonlinear rectification behavior that will be of interest to the electronic industry.

**Acknowledgment.** We acknowledge the interconnect focus center New York (FC-NY) and a faculty grant development from NYSTAR, NY, for funding support.

**Supporting Information Available:** N 1s core-level spectra recorded from a porous gold nanoparticle film deposited on a copper substrate. This material is available free of charge via the Internet at <http://pubs.acs.org>.

LA060869G

---

(12) Fan, H.; Yang, K.; Boye, D. M.; Sigmon, T.; Malloy, K. J.; Xu, H.; Lopez, G. P.; Brinker, C. J. *Science* **2004**, *304*, 567.